



Research Paper / Makale

The Shielding Parameters of the Superconducting Tin Based Solders

Canan AKSOY^{1a}

*Electronics and Communication Engineering, Faculty of Technology, Karadeniz Technical University, 61830, Of, Trabzon, TURKEY
cananaksoy@ktu.edu.tr

Received/Geliş: 07.07.2021

Accepted/Kabul: 11.08.2021

Abstract: In the current study shielding parameters, the mass and linear attenuation coefficients, and half value layer (HVL), tenth value layer (TVL) and mean free path (MFP) values were calculated theoretically used the calculation software Phy-X/PSD for superconducting lead free SnIn alloy solder system that the alloy composition were chosen from the binary phase diagram of SnIn and PbSn which has been mostly used solder alloy for in micro electric and cryogenic applications for decades. The results showed that among the studied sample increasing tin content decreases the shielding efficiency and Sn₂₀In₈₀ system shows better shielding properties depend on the used energy. Thus, it needs to be considered the energy range to determine the thickness of the material subjected to the gamma radiation as the shielding parameters change depend on using energy

Keywords: Attenuation coefficient, Phy-X/PSD, superconductors, solder alloys

Kalay Tabanlı Süperiletken Lehim Alaşımlarının Zırhlama Parametreleri

Öz: Mevcut çalışmada zırhlama parametreleri, kütle ve lineer zayıflama katsayıları ile yarı değer kalınlık, (HVL), onda bir kalınlık değeri (TVL) ve ortalama serbest yol (MFP) değerleri teorik olarak Phy-X/PSD hesaplama yazılımı kullanılarak hesaplanmıştır. Süper iletken kurşunsuz SnIn lehim sistemi için, SnIn kompozisyonu değerleri, ikili faz diyagramından yararlanılarak seçildi ve çoğunlukla mikro elektrik ve kriyojenik uygulamalarda onlarca yıldır lehim olarak kullanılan PbSn alaşımı kullanıldı. Çalışmanın sonuçları, incelenen numunelerde artan kalay içeriğinin koruma verimliliğini azalttığını ve Sn₂₀In₈₀ sisteminin kullanılan enerjiye bağlı olarak daha iyi zırhlama özellikleri gösterdiğini ortaya koymuştur. Bu nedenle, zırhlama parametreleri enerji kullanımına bağlı olarak değiştiğinden, gama radyasyonuna maruz kalan malzemenin kalınlığını belirlemek için enerji aralığının dikkate alınması gerekir.

Anahtar Kelimeler: Zayıflama katsayısı, Phy-X/PSD, süper iletkenler, lehim alaşımları

1. Introduction

Solder materials are quite crucial for microelectric, superconducting, aerospace application for connecting materials. In the current technology, lead based solders are mostly used however the solder technology has been moved away to prefer lead free solders due to harmful effect of Lead on environmental and human health with the restriction of ROHS and WHEE directives [1,2]. The researchers have been investigating novel lead free solders. Tin based solders can be replaced of lead based solders as Tin has adequate mechanical properties such as high ductility, low melting point and it has also good electrical and superconducting properties. The lead free solders may be used in the technology that are not useful for superconducting applications though they may be used for aerospace applications [3]. Tin based solders such as SnIn and SnInBi can be new candidates for

How to cite this article

Aksoy C., "The shielding Parameters of the Tin Based Solders" El-Cezeri Journal of Science and Engineering, 2021, 8(3); 1529-1535.

Bu makaleye atıf yapmak için

Aksoy C., "Kalay Tabanlı Süperiletken Lehim Alaşımlarının Zırhlama Parametreleri" El-Cezeri Fen ve Mühendislik Dergisi 2021, 8(3); 1529-1535.
ORCID ID: 0000-0003-3738-6886

superconducting applications although the critical current of the solders are lower than the lead based solders [4]. The other parameters need to be considered such as shielding parameters which are used to determine the attenuated radiation of the media and thickness for the new developed materials, or they are currently used for designing of shielded materials. These parameters are the mass and linear attenuation coefficients, and half value layer (HVL), tenth value layer (TVL) and mean free path (MFP). They are evaluated for composite materials [5], bulk and alloy materials [6, 7, 8], soil sample [9], minerals [10], for several elements [11]. These parameters also need to be investigated for the superconducting solders as they have been used in the high magnetic system and nuclear fusion reactors.

The main objective of this study is determining the shielding parameters of the binary SnIn solder system and SnPb (60:40) solders. They were investigated by using the calculation software Phy-X/PSD [12] values for the photon energy range from 10^{-3} to 10^3 MeV and compared the shielding abilities of the SnIn solders with the PbSn solder.

2. Material and Method

The SnIn alloy (the selected compositions are Pb:Sn; 20:80,35:65,45:55,65:35,75:25) and SnPb (60:40) were chosen from the SnIn binary phase diagram as seen in Figure 1 which shows the β (In rich), $\beta + \gamma$ (mixed state), γ (Sn rich) phases and T_c is the superconducting transition temperature of the phases for β and γ phases. Phase evaluation of the chosen solders, microstructural and superconducting properties were given in the previous published studies [4,13]

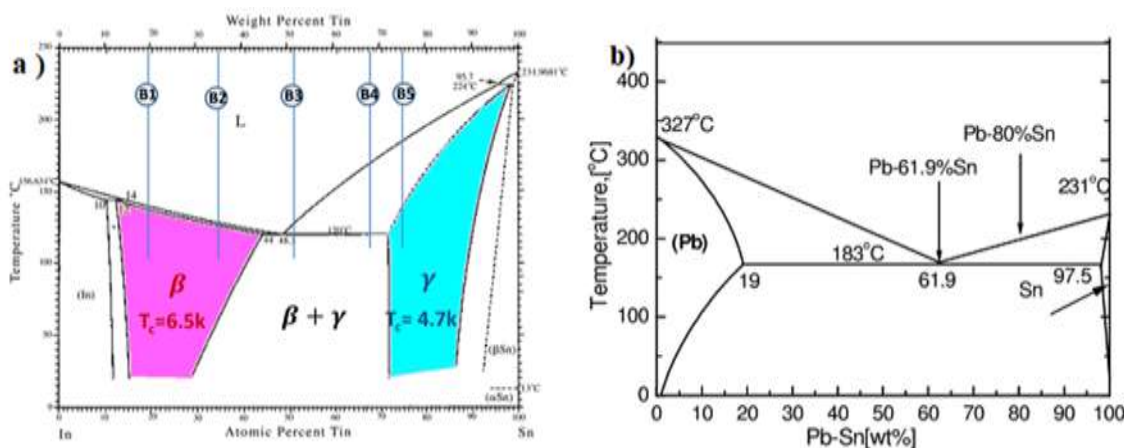


Figure 1. a) Phase diagram of binary SnIn [13] alloys and (b) Phase diagram of PbSn alloy [14].

The densities of the Sn and In are the same as 7.31g/cm^3 [15]. The coding and the chemical compositions (wt %) and densities (g/cm^3) of the investigated binary systems are given in Table 1

Table 1. The coding, chemical compositions (wt %) and densities of the solder systems

Chemical Composition	Code	Density (g/cm^3)
$\text{Sn}_{20}\text{In}_{80}$	S1	7.31
$\text{Sn}_{35}\text{In}_{65}$	S2	7.31
$\text{Sn}_{45}\text{In}_{55}$	S3	7.31
$\text{Sn}_{65}\text{In}_{35}$	S4	7.31
$\text{Sn}_{75}\text{In}_{25}$	S5	7.31
$\text{Sn}_{60}\text{Pb}_{40}$	S6	8.37

The shielding parameters are calculated by considered the Beer-Lambert's Law. It was proved that if a gamma-ray passes through an x-thickness material the incident beam intensity is attenuated as formulated Equation 1.

$$I = I_0 e^{-\mu x} \quad (1)$$

where I_0 is incident photon intensity, I is passed photon intensity of the absorbent material, and μ (cm^{-1}) is the linear attenuation coefficient of the material.

The attenuation coefficients (μ/ρ) of the samples is calculated by using the mixture rule Eq. (2):

$$\mu/\rho = \sum_i w_i (\mu/\rho)_i \quad (2)$$

where ρ is the density of the alloy, while w_i and $(\mu/\rho)_i$ are the weight fraction and mass attenuation coefficient values of the i th constituent element in alloy, respectively [16,18].

Theoretical Mass Attenuation Coefficient (μ/ρ) of alloy samples was calculated using the software [17, 19, 20].

The Half-Value Layer (HVL) shows the thickness of the shield the half weakened density of incident photon, the tenth value layer (TVL) is the thickness of a required shield for attenuated radiation beam to ten percent of the radiation level and mean free path (MFP) is the material thickness, reducing the initial radiation intensity to 36,8% after passing through the absorber. HVL, TVL, MFP are calculated as following [21, 22];

$$HVL = \ln 2 / \mu \quad (3)$$

$$TVL = \ln 10 / \mu \quad (4)$$

$$MFP = \frac{\int_0^{\infty} t e^{-\mu t} dt}{\int_0^{\infty} t e^{-\mu t} dt} = \frac{1}{\mu} \quad (5)$$

3. Results and Discussion

The superconducting binary SnIn and PbSn systems were investigated in terms of shielding parameters by using Phy-X/PSD software programme. The density of the materials was used for running the programme. The figures were plotted by Origin 9 version. The mostly used solder in the current technology is PbSn. Thus, the plots were designed by comparing the studied sample SnIn and PbSn solder systems.

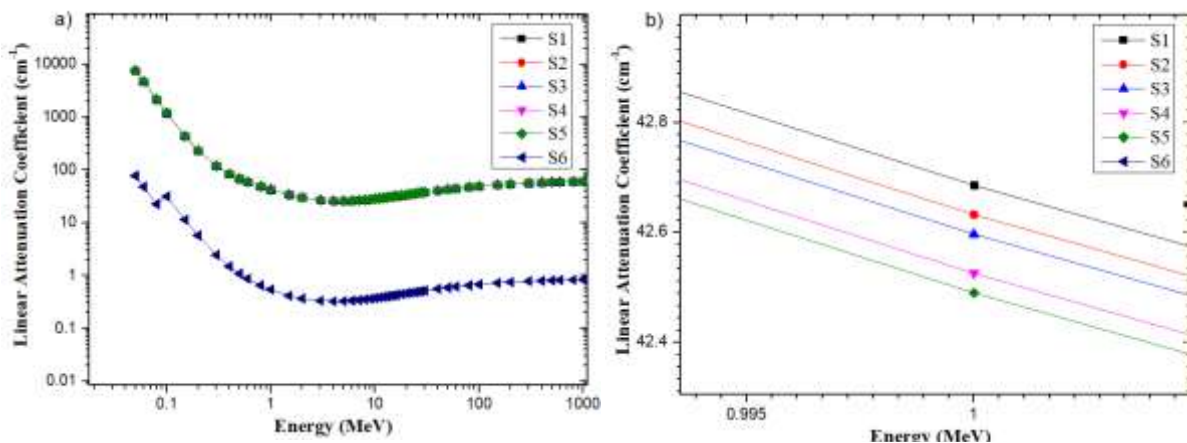


Figure 2. Linear attenuation coefficient values as a function of Energy for studied samples b) Inset plot show the difference from the S1 to S5 samples

The mass attenuation coefficients (μ/ρ), linear attenuation coefficient, the half value layer (HVL), tenth value layer (TVL) and the mean free path (MFP) values were calculated theoretically for the energy range from 10^{-3} to 10^3 MeV. Fig. 2 shows the variations of total μ/ρ values for SnIn and PbSn solder systems rely on the photon energies, linear attenuation coefficient of the SnIn samples are higher than the SnPb solder system. Among the SnIn solder alloys, it is clear that the increasing Sn content induce the decreasing of the linear attenuation coefficient. Namely, S1 has the highest S5 has the lowest linear attenuation values. However, lead addition to Sn (S6) reduced the linear attenuation coefficient. As seen in the inserted graph of Fig.1. Additionally, in the low energies, μ/ρ values has large number but by increasing energy it is reducing for the current samples. This may be explained with the photonic interactions such as photoelectric absorption mechanism in low energies and Compton scattering in intermediate energies and pair production in high energies [21].

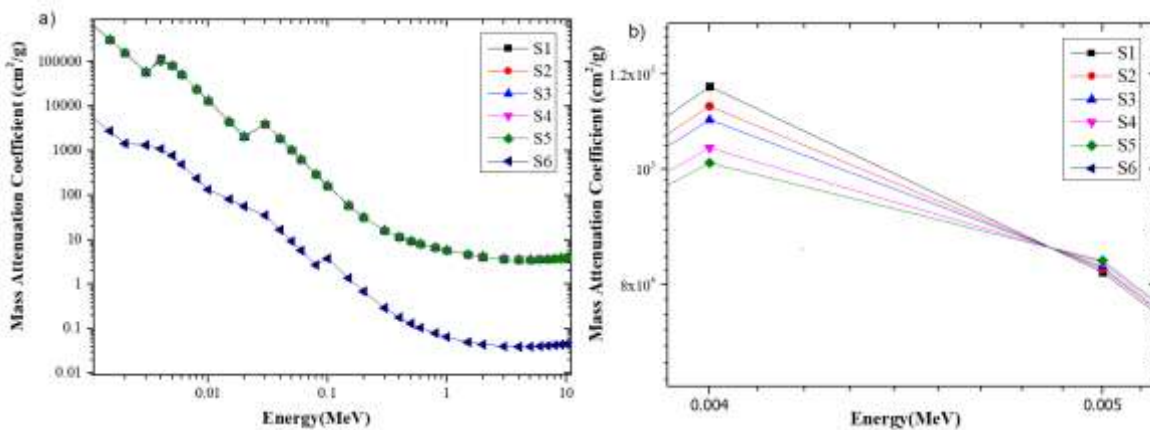


Figure 3. Mass attenuation coefficient values as a function of Energy b) Inset plot show the difference from S1 to S5 samples

Fig.3 presented the mass attenuation coefficient of the studied sample. Similar of the linear attenuation coefficient, increasing Sn content caused of decreasing the mass attenuation coefficient. Below of 0.005 MeV, S1 showed the highest S5 showed the lowest values but they are changing opposite order to highest one was S5 and the lowest one was S1 after $E > 0.005$ MeV. As comparing the SnIn and PbSn systems, S6 showed the highest value.

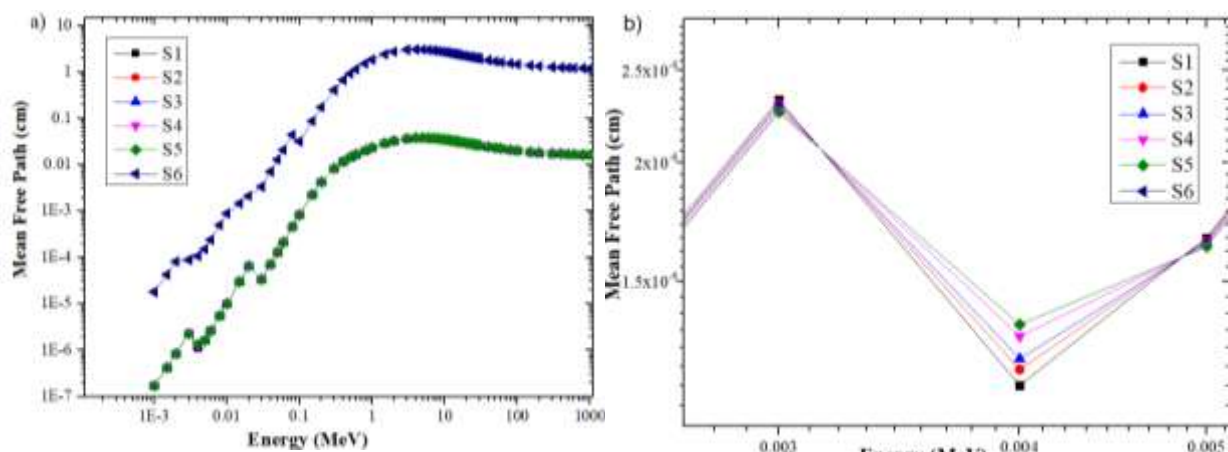


Figure 3. a) The mean free path as a function of energy for the studied samples b) Focused plot shows the comparison of the SnIn system in the certain energy range

The variation of MFP for solder systems against photon energies were shown in the Fig.3. Apparently, it is seen that, the values are increasing gradually up to $E < 0.1$ MeV energy and after 7 MeV, it is decreasing and the MFP showed nearly constant after 10 MeV energy. The SnIn alloys

have lower MFP values than the PbSn solder system. Among the SnIn alloys, S1 indicates the lower MFP according to inserted plot in Fig.3, though the values are quite close. To determine the best attenuate performance of the solder system, it can be claimed that smaller values are much more acceptable for shielding [22]. So, among the all samples, S1 shows the best performance for shielding $E > \text{MeV}$.

TVL values are enhancing by increasing photon energy till 1MeV and after it is decreasing and stabilising with the increasing energy as demonstrated in Fig.4. Among the all samples, up to 0.003MeV energy, S6 shows the highest value and S1 show the lowest value. However, after this energy it turns to vise a versa, namely it is clearly seen at 0.03 MeV energy, S1 shows the highest and S6 shows the lowest TVL values. Hence, it can be said that depending on the energy, the shielding superiority decreases with the enhancing the Sn content for SnIn solder system.

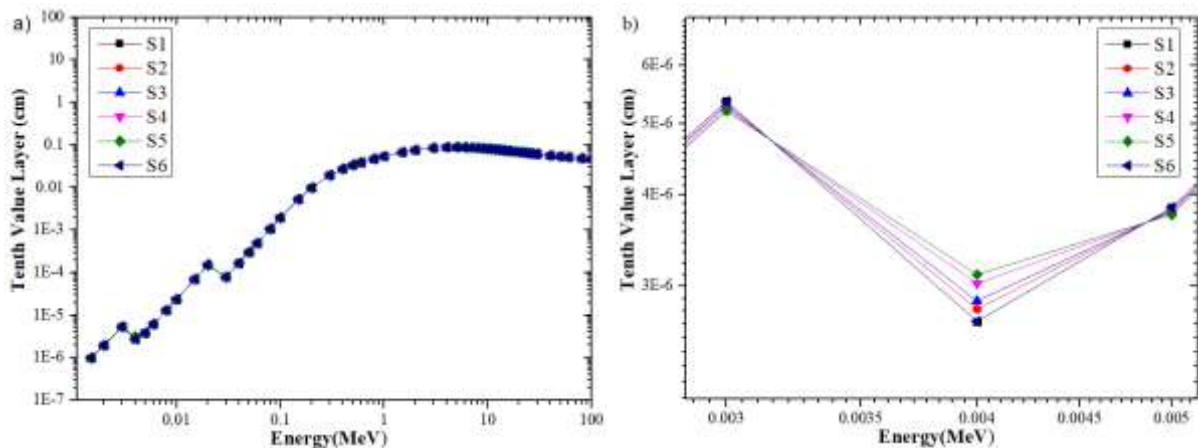


Figure 4. The TVL as a function of Energy for the solder system were presented and b) Inserted plot showed the comparison of SnIn and PbSn system at between the certain energy levels

The HVL thickness can be used while determining the sample thickness as it shows the transmitted intensity. It is half value of the incident intensity of gamma radiation and it depends on linear attenuation coefficient value (μ). In the current samples, Fig. 5 shows the HVL as a function of the energy, S6 has the highest HVL thickness value and among the SnIn alloy system, S1 has the lowest HVL at 0.004 MeV, however, S5 has the lowest value till to 0.003 MeV but after this energy S5 has the highest HVL to 0.005 MeV, upward of this energy again the order is changing to highest S1 as seen Fig.5b. Thus, it needs to be considered the energy range to determine the thickness of the material subjected to the gamma radiation.

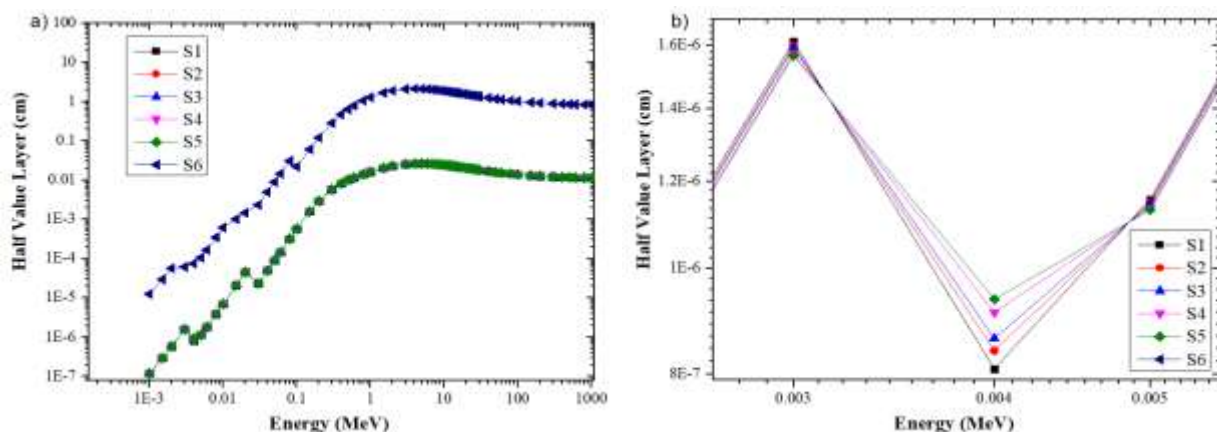


Figure 5. a) The HVL as a function of Energy for the solder systems b) Focused plot showed the comparison of the SnIn system in terms of energy range

2. Conclusion

In the current study, the shielding parameters such as the mass and linear attenuation coefficients, and half value Layer (HVL), tenth value layer (TVL) and mean free path (MFP) were calculated by using the calculation software Phy-X/PSD for SnIn and PbSn solder system. According to the calculated data it can be said that S1 has better shielding properties for the energy range of $E > 0.003$ MeV but lower than these energies S6 has better shielding properties. This data may be useful for various applications for designing the materials by considering the radiation shielding

Authors' Contributions

CA carried out the study, designed and wrote up the article. The author read and approved the final version of the paper.

Competing Interests

The author declares that there is no competing interests.

References

- [1]. Directive 2002/95/EC on the restriction of the use of certain hazardous substances in electrical and electronic equipment. European Parliament and the Council of 27 January 2003 (OJ L 37. 13.2.2003. p. 19)
- [2]. Directive 2002/96/EC on waste electrical and electronic equipment. European Parliament and the Council of 27 January 2003 (OJ L 37. 13.2.2003. p. 24)
- [3]. Aksoy, C., Mousavi T., Brittles G., Grovenor C. R. M., and Speller S. C., "Lead-free solders for superconducting applications", IEEE Transactions on Applied Superconductivity, 2016, 26(3):1-3.
- [4]. Mousavi T., Aksoy. C., Grovenor C. R. M. & Speller S. C., "Microstructure and superconducting properties of Sn–In and Sn–In–Bi alloys as Pb-free superconducting solders", Superconductor Science and Technology, 2015, 29(1): 015012.
- [5]. Sürücü, A.M and Subaşı S., "Nanomateriyallerin Kompozit Malzemelerin Radyasyon Zırhlama Özelliklerine Etkisinin İncelenmesi", El-Cezeri Journal of Science and Engineering, 2021, 8(1): 182-1941.
- [6]. Sirin, M., "The effect of titanium (Ti) additive on radiation shielding efficiency of $Al_{25}Zn$ alloy, Progress in Nuclear Energy", 2020, 128:103470.
- [7]. Karadoğan I. Z., Özdemir, Y., Kavaz, E., "Ni Tabanlı Bazı Süperalaşımın Foton Etkileşim Özelliklerinin İncelenmesi", El-Cezeri Journal of Science and Engineering, 2021, 8(2):552-566.
- [8]. Aksoy, C., "The X-Ray fluorescence parameters and radiation shielding efficiency of silver doped superconducting alloys", Radiation Physics and Chemistry, 2021,86: 109543.
- [9]. Sarı S., Dizman S., "Ovit Dağbaşı Gölü Çevresinden Alınan Toprak Örneklerinde Radyoaktivite ve Radyolojik Etkilerin Araştırılması", El-Cezeri Journal of Science and Engineering, 2020, 7(3):1122-1130.
- [10]. Baltas, H., Sirin, M., Celik, A., Ustabas, & El-Khayatt, A. M., "Radiation shielding properties of mortars with minerals and ores additives", Cement and Concrete Composites, 2019, 97: 268-278.
- [11]. Kaya, N., Tıraşoğlu, E., Apaydın, G., Aylıkçı, V., & Cengiz, E. "K-shell absorption jump factors and jump ratios in elements between Tm (Z=69) and Os (Z= 76) derived from new mass attenuation coefficient measurements", Nuclear Instruments and Methods in Physics Research Section B: Beam Interactions with Materials and Atoms, 2007, 262(1):16-23.

- [12]. Şakar E., Özpolat Ö.F., Alim B., Sayyed M.I., Kurudirek M., “Phy-X/PSD: development of a user friendly online software for calculation of parameters relevant to radiation shielding and dosimetry”, *Radiation Physics and Chemistry*, 2020,166:108496.
- [13]. Mousavi, T., Aksoy, C., Grovenor, C., & Speller, S., “Phase evolution of superconducting Sn–In–Bi solder alloys”, *IEEE Transactions on Applied Superconductivity*, 2016, 26(3): 1-4.
- [14]. Xi, Y., Lan-jun L., Fang-Q. Z., and Zhi-hao C., “Effect of Temperature-induced Discontinuous Liquid Structure Change on the Solidification Behaviour and Solidified Structures of Pb-Sn” Alloy [J], 2004, *Foundry*.
- [15]. “Density of Sn and In elements”, <https://www.angstromsciences.com/density-elements-chart>. 05.07.2021.
- [16]. Hubbell J.H., Seltzer S.M., “Tables of X-ray mass attenuation coefficients from 1 keV to 20 MeV for elements Z=1–92”, National Institute of Standards and Technology (IR) Report, 1995, 5632.
- [17]. Berger M.J., Hubbell J.H., “XCOM: Photon Cross Sections Database. Web Version 1.2., National Institute of Standards and Technology, Gaithersburg, MD 20899, USA, 1999 (originally published as NBSIR 87-3597, XCOM: Photon Cross Sections on a Personal Computer”, 1987:1987–1999.
- [18]. Jackson D.F., Hawkes D.J., “X-ray Attenuation Coefficients of Elements and Mixtures, *Physics Reports*”, 1981, 70(3):169-233.
- [19]. Gerward L., Guilbert N., Jensen K.B., Leving H., “WinXCom- a program for calculating X-ray attenuation coefficients”, *Radiation physics and chemistry*, 2004, 71: 653-4.
- [20]. Gerward L., Guilbert N., Jensen K.B., “Levring H., X-ray absorption in matter, *Reengineering XCOM. Radiation Physics and Chemistry*”, 2001, 60(1-2):23-4.
- [21]. Mariyappan M., Marimuthu K., Sayyed M.I., Dong M.G., Kara U., “Effect Bi₂O₃ on the physical, structural and radiation shielding properties of Er³⁺ ions doped bismuth sodium fluoroborate glasses”, *J. Non-Cryst. Solids*, 2018, 499:75–85
- [22]. Açar, O., “Investigation on Gamma Radiation Shielding Behaviour of CdO–WO₃–TeO₂ Glasses from 0.015 to 10 MeV”, *Cumhuriyet Science Journal*, 2018, 39(4):983-990.